Device Fabrication for High Precision Electrical Transport Measurements on Complex Oxide Thin Films

Betty Hu[1], Jacob Ruf[2], Kyle Shen[2]

[1] Department of Applied Physics and Applied Mathematics, Columbia University, New York, NY 10027

[2] Department of Physics, Cornell University, Ithaca, NY, 14853

Abstract:

The open shell configuration of transition metal cations and quantum interactions between electrons can give rise to novel and unexpected electronic properties in transition-metal oxides (TMOs). For example, the Ruddlesden-Popper ruthenate family of materials ($A_{n+1}Ru_nO_{3n+1}$, where A = Ca, Sr, Ba is an alkaline earth element), are known to exhibit a wide array of electronic ground states in the bulk, ranging from ferromagnetic metals ($SrRuO_3$, $BaRuO_3$) [1][2] in the three-dimensional limit (n = ∞), to antiferromagnetic Mott insulators (Ca_2RuO_4) [3] and unconventional superconductors (Sr_2RuO_4) [4] in quasi-two-dimensional single-layer (n = 1) compounds. This sensitivity of electronic and magnetic properties to subtle changes in crystal structure suggests that the former can be artificially "tuned" in thin films grown by molecular-beam epitaxy (MBE) by adjusting parameters that couple to the film crystal structure, such as the structure and orientation of the substrate on which the film is deposited. Besides providing a useful platform for studying fundamental problems in solid-state physics, understanding how to exploit these structure-property relationships in TMOs is a crucial step towards the broader goal of realizing emergent properties of correlated electrons—e.g. metal-insulator transitions, magnetism, and superconductivity—in targeted materials by design. This project focuses on using electrical transport measurements to characterize the interfacial electronic structure of calcium ruthenate thin films grown by MBE. In particular, photolithography methods are used to pattern devices on the surfaces of films to enable more directionally-precise transport measurements.

Introduction:

The Ruddlesden-Popper family of calcium ruthenates ($Ca_{n+1}Ru_nO_{3n+1}$) are an interesting class of TMOs to study because of the rich diversity of electronic ground states they exhibit: in the bulk, the three-dimensional end member $CaRuO_3$ is a paramagnetic metal [5], while the quasi-two-dimensional end member Ca_2RuO_4 is an antiferromagnetic Mott insulator that undergoes a thermal metal-insulator transition near room temperature ($T \sim 350$ K) [6]. Because the low-energy electronic and magnetic properties of $Ca_{n+1}Ru_nO_{3n+1}$ strongly depend on the crystal structure, these ruthenates present an ideal materials platform to explore how tweaking the latter can induce large changes in the former. Versatile thin-film deposition methods such as molecular-beam epitaxy (MBE) allow a high degree of control over the film crystal structure via “knobs” such as the choice of substrate, which serves as a

template for the subsequent film growth and can impose variable amounts of strain on the atoms in the film.

Following film growth, transport measurements conducted using a four-point probe method are a useful technique to study the interfacial electronic properties of films. With large-area square samples, the easiest method of conducting four-point probe measurements is to place the voltage and current contacts on the four corners of the sample, in the so-called Van der Pauw configuration [7]. However, for materials with anisotropic crystal structures, measurements taken using this method represent a coarse average between the properties in the two mutually perpendicular in-plane directions, which can sometimes vary considerably.

One way to resolve these intrinsic anisotropies is by using photolithography techniques to fabricate gold devices—"Hall bars"—on the surface of a material to take measurements on. Hall bar measurements can be taken over a smaller area and in a specific direction.

In this project, Hall bars have been fabricated on the surfaces of both $CaRuO_3$ and Ca_2RuO_4 samples grown on $LaAlO_3$ substrates by molecular-beam epitaxy. $LaAlO_3$ is chosen in particular because resistivity measurements of Ca_2RuO_4/ $LaAlO_3$ show two metal-insulator transitions between 300 K and 4 K, suggesting this system is in close proximity to the electronic ordering instability observed in bulk Ca_2RuO_4. Thus, performing temperature-dependent transport measurements on these calcium ruthenate samples promises to enhance our understanding of the metal-insulator transition observed in calcium ruthenates, both between $CaRuO_3$ and Ca_2RuO_4, and within Ca_2RuO_4 itself.

Device Fabrication Process:

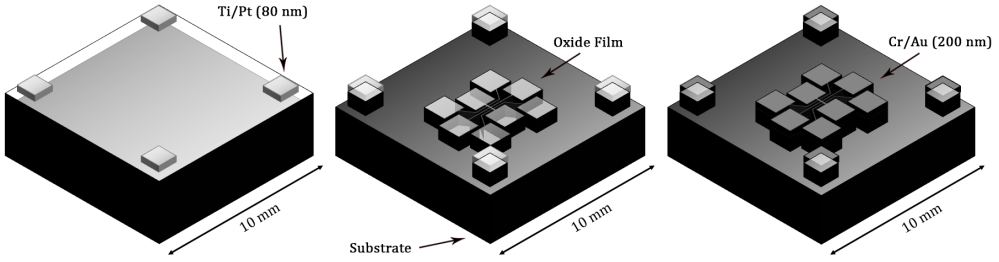

Figure 1a *Figure 1b* *Figure 1c*

Hall bars were fabricated in a three-layer process using photolithography techniques, shown schematically in Figure 1. Prior to starting any fabrication, a four-point probe resistivity measurement was taken on each sample from 300 K to 4 K in Van der Pauw geometry to serve as a reference for later transport measurements.

The purpose of the first layer, shown in Figure 1a, was solely to place alignment marks on the sample. A layer of AZ nLOF 2020 photoresist, a negative photoresist, was patterned on each 1 cm^2 square sample. 15 nm of titanium and 65 nm of platinum were then deposited

on the surface using e-beam evaporation and lifted off using acetone, leaving titanium and platinum alignment marks on the surface of the film.

In the second layer, shown in Figure 1b, SPR220-3.0 photoresist, a positive photoresist, was patterned to leave resist on the sample only where there would eventually be Hall bars. An ion milling machine was then used to etch away all exposed film from the surface of the sample, exposing the substrate. Because the photoresist was much thicker than the film, it prevented the film underneath from being etched away as well. The remaining photoresist was then removed using acetone before starting the third layer.

In the third layer, shown in Figure 1c, AZ nLOF 2020 photoresist was patterned to expose the surface of the sample only where there would eventually be Hall bars, aside from a 20x120 μm strip on each bar that connected the two current pads. 20 nm of chromium and 200 nm of gold were then deposited on the surface using e-beam evaporation and lifted off using acetone.

Each film, after fabrication was completed, had 34 devices patterned on its surface (perpendicular to the film growth direction) in four different orientations. 12 each were parallel to the edges of the substrate, and five each were at two intermediate angles.

Conducting Measurements:

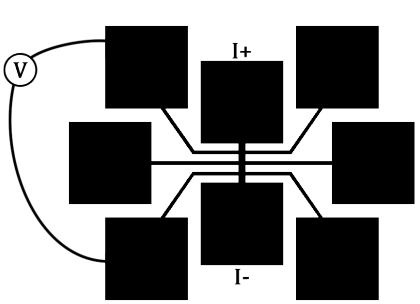

Figure 2a

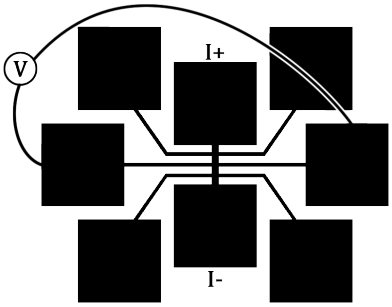

Figure 2b

Each Hall bar (Figure 2) contains eight 250x250 μm contact pads, with two serving as current contacts and six as voltage contacts. An exposed 20x120 μm strip of film connects the two current pads, and all other connecting lines are 10 μm wide.

Patterned samples were placed on a chuck compatible with the Quantum Design Physical Property Measurement System (PPMS). Electrical connections were made from the contact pads of the Hall bars to those of the PPMS chuck using aluminum wire bonding. The design of each Hall bar allowed for both longitudinal and transverse measurements of resistivity to be taken by wire bonding to specific contact pads as shown in Figures 2a and 2b, respectively. Measurements were taken using an alternating drive current with a lock-in amplifier.

Zero-field longitudinal resistivity measurements were taken on each sample from 300 K to 4 K, while cooling and warming, to compare against baseline resistivity measurements

taken prior to device patterning. Temperature-dependent Hall effect measurements of transverse resistivity were also performed on each sample under an externally applied perpendicular magnetic field at various temperature stops.

Results & Discussion:

Figure 3a

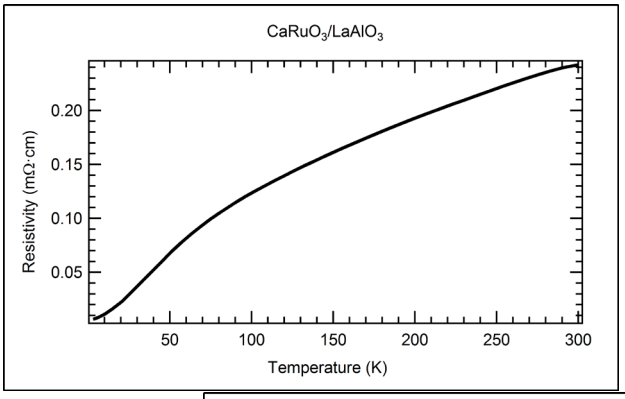

Figure 3b

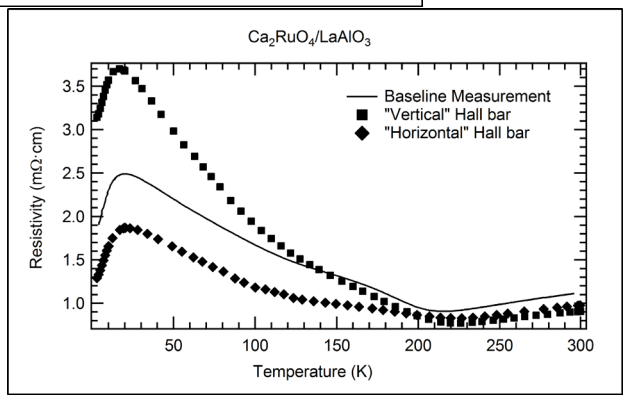

Zero-field longitudinal resistivity versus temperature (ρ vs. *T*) measurements were taken for $CaRuO_3/LaAlO_3$ and $Ca_2RuO_4/LaAlO_3$, shown in Figures 3a and 3b, respectively, on multiple Hall bars to compare against baseline measurements taken prior to starting any fabrication. No significant difference was found between baseline measurements, “vertical” Hall bar measurements, and “horizontal” Hall bar measurements on $CaRuO_3/LaAlO_3$.

Resistivity versus temperature measurements taken on “vertical” and “horizontal” Hall bars on $Ca_2RuO_4/LaAlO_3$ were found to be higher and lower than baseline measurements, respectively. For all resistivity measurements on $Ca_2RuO_4/LaAlO_3$, two metal-insulator transitions—indicated by changes in the sign of the derivative dρ/dT—were observed at 20 K and 200 K.

Figure 4a *Figure 4b*

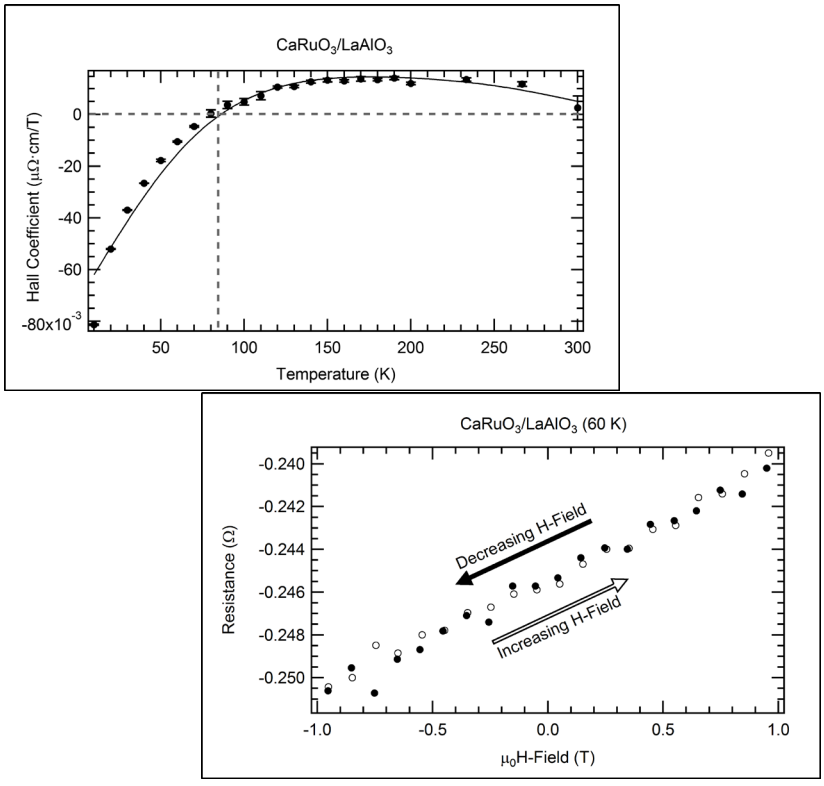

Figure 4a shows values of the Hall coefficient versus temperature (R_H vs. T) for $CaRuO_3/LaAlO_3$ calculated from the slope of the transverse resistance R_{xy} under a variable externally applied magnetic field H. As shown in Figure 4b, R_{xy} was completely reversible for the $CaRuO_3/LaAlO_3$ sample, independent of the field sweep direction. A sign change in

R_H was observed around 80 K, indicating a change from predominantly electrons as charge carriers below 80 K to predominantly holes as charge carriers above 80 K.

Figure 5a

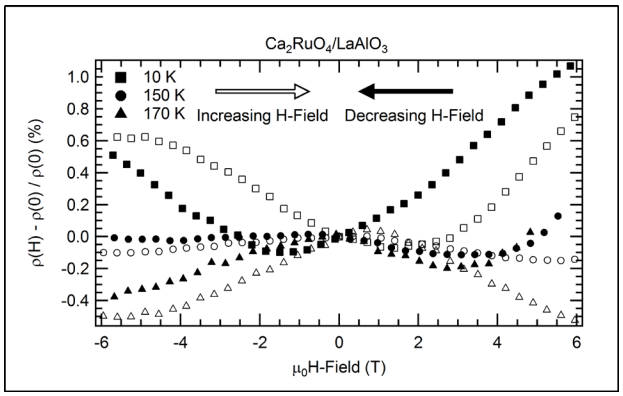

Figure 5b

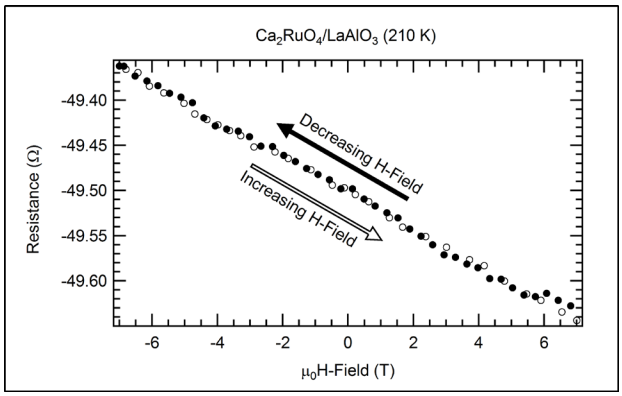

Hall effect measurements conducted on $Ca_2RuO_4/LaAlO_3$ yielded much different results. Non-linear response of the transverse resistivity to the applied *H* field is shown in Figure 5a at 10 K, 150 K, and 170 K, and is characteristic of a so-called "anomalous Hall effect", which is often observed in magnetically ordered materials with appreciable spin-orbit coupling. Notably, this hysteretic and non-linear behavior of ρ vs. *H* (1) was not observed in paramagnetic $CaRuO_3/LaAlO_3$ at any temperatures, and (2) was only present in $Ca_2RuO_4/LaAlO_3$ below the metal-insulator transition at 200 K. In Hall effect measurements conducted at 210 K, shown in Figure 5b, ρ showed no dependence on the *H*-field sweep direction.

Conclusions:

Based off the observation of hysteretic and non-linear behavior of ρ vs. *H* in $Ca_2RuO_4/LaAlO_3$ below the metal-insulator transition at 200 K, it is very likely that the metal-insulator transition is accompanied by the formation of canted antiferromagnetic order.

Future Work:

Further data should be taken on $Ca_2RuO_4/LaAlO_3$ samples to confirm trends that were noticed in this project—namely, the directional-dependency of Hall bars observed in both resistivity and Hall effect measurements, as well as the dependency on the magnetic field sweep direction seen in Hall effect measurements. Because it's known that sample uniformity is generally best in the center of samples grown by MBE, more measurements should be conducted on different Hall bars across a single sample to see how the results vary depending on each Hall bar's position within a sample. Measurements should also be conducted on different $Ca_2RuO_4/LaAlO_3$ samples to confirm that the observed temperature- and field-dependent changes in resistivity are intrinsic properties of the films and did not arise out of either the process of fabricating devices or the process of preparing for and taking measurements. Longitudinal magnetoresistance measurements should be performed on Hall bars as well to gain further insight about the nature of the magnetically ordered state and its relationship to the crystal structure of epitaxially strained Ca_2RuO_4.

Acknowledgements:

This material is based upon work supported by the National Science Foundation (Platform for the Accelerated Realization, Analysis, and Discovery of Interface Materials (PARADIM) under Cooperative Agreement No. DMR-1539918.

References:

[1] J. M. Longo, P. M. Raccah, and J. B. Goodenough, J. Appl. Phys. **39**, 1327 (1968).

[2] J.-S. Zhou, K. Matsubayashi, Y. Uwatoko, C.-Q. Jin, J.-G. Cheng, J. B. Goodenough, Q. Q. Liu, T. Katsura, A. Shatskiy, and E. Ito, Phys. Rev. Lett. **101**, 077206 (2008).

[3] S. Nakatsuji, S. Ikeda, and Y. Maeno, J. Phys. Soc. Jpn. **66**, 1868-1871 (1997).

[4] K. Ishida, H. Mukuda, Y. Kitaoka, K. Asayama, Z. Q. Mao, Y. Mori and Y. Maeno, Nature. **396**, 658-660 (1998).

[5] T. He and R. J. Cava, Phys. Rev. B. **63**, 172403 (2001).

[6] M. Braden, G. André, S. Nakatsuji, and Y. Maeno, Phys. Rev. B. **58**, 847 (1998).

[7] L. J. van der Pauw, Philips Technical Review. **20**, 220-224 (1958).